JOC The Journal of Organic Chemistry

pubs.acs.org/joc Featured Article

Application of Transition-Metal Catalysis, Biocatalysis, and Flow Chemistry as State-of-the-Art Technologies in the Synthesis of LCZ696

Xingxian Gu, Jibin Zhao, Like Chen, Yunzhong Li, Bo Yu, Xiangguang Tian, Zhongcheng Min, Su Xu, Huijuan Gu, Junjie Sun, Xiaoquan Lu, Meng Chang, Xufan Wang, Liqun Zhao, Shengqing Ye, Hongwei Yang, Yingtao Tian, Feng Gao, Yu Gai, Guanghua Jia, Jingjing Wu, Yan Wang, Jianghua Zhang, Xuesong Zhang, Weichun Liu, Xin Gu, Xi Luo, Hai Dong, Huaimin Wang, Berthold Schenkel, Francesco Venturoni, Paolo Filipponi, Bertrand Guelat, Thomas Allmendinger, Bernhard Wietfeld, Pascale Hoehn, Nikola Kovacic, Luca Hermann, Thierry Schlama, Thomas Ruch, Nadine Derrien, Philippe Piechon, and Florian Kleinbeck*

Cite This: https://dx.doi.org/10.1021/acs.joc.0c00473 Read Online

ACCESS | Metrics & More | Article Recommendations | Supporting Information

ABSTRACT: LCZ696 is a novel treatment for patients suffering from heart failure that combines the two active pharmaceutical ingredients sacubitril and valsartan in a single chemical compound. While valsartan is an established drug substance, a new manufacturing process suitable for large-scale commercial production had to be developed for sacubitril. The use of chemocatalysis, biocatalysis, and flow chemistry as state-of-the-art technologies allowed to efficiently build up the structure of sacubitril and achieve the defined performance targets.

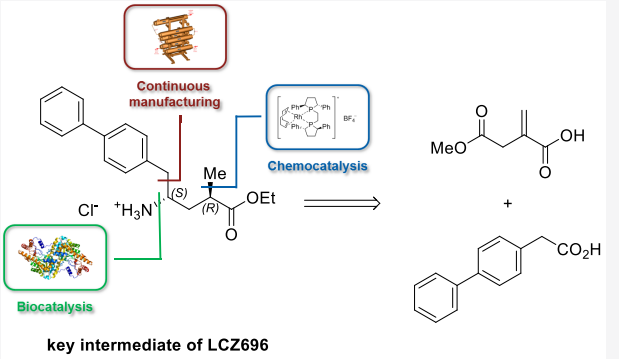

INTRODUCTION

LCZ696 (**1**, sacubitril valsartan sodium hydrate) is indicated for the treatment of heart failure in patients with systolic dysfunction. A total of 1.0 million patients are hospitalized each year in the US and in Europe due to heart failure, corresponding to approximately 5% of all acute hospital admissions.[1] The overall five year survival rate for heart failure is as poor as or worse than those for advanced cancer or stroke patients.[1b] Heart failure therefore represents a major public health problem associated with a high mortality rate, frequent hospitalizations, and poor quality of life.

In the PARADIGM-HF clinical trial, a Phase 3 clinical trial involving more than 8000 patients worldwide, LCZ696 was compared to enalapril, an angiotension-converting enzyme (ACE) inhibitor considered as the standard of care at the time.[2] The PARADIGM-HF clinical trial was designed to determine if treatment with LCZ696 could provide a greater benefit in cardiovascular mortality and morbidity reduction. In 2014, the trial was stopped before the originally planned end date due to the overwhelmingly positive results. Introduction of LCZ696 has therefore widely been described as a paradigm shift in the treatment of heart failure.[2b]

LCZ696 is a supramolecular complex that combines the two individual active components—sacubitril and valsartan—in their anionic forms.[3] Besides sacubitril and valsartan in a 1:1 ratio, sodium cations and water are part of the crystalline LCZ696 complex, which has a hexameric unit cell (Figure 1). Water forms an essential component of the crystal structure, leading to the creation of an extensive hydrogen-bonding network.

While valsartan as an established drug substance is manufactured according to highly optimized manufacturing processes,[4] sacubitril represents a new molecular entity that is not independently marketed as a drug substance. During late-phase process development, activities therefore focused on the development of a manufacturing process for sacubitril that was suitable to address the supply for Phase 3 clinical studies and

Received: February 22, 2020

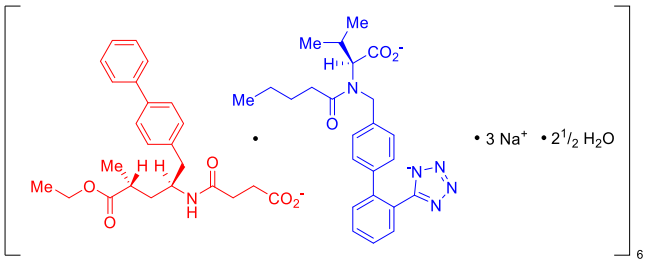

LCZ696 (sacubitril valsartan sodium hydrate)

Figure 1. Structure of LCZ696 (sacubitril valsartan sodium hydrate); structure of sacubitril shown in red, structure of valsartan shown in blue.

initial market supply.[5] Starting from protected (*R*)-biphenyl alaninol (**1**), accessed itself in five chemical transformations, the core structure of sacubitril as represented in key intermediate **6** could be quickly assembled. TEMPO-catalyzed oxidation of alcohol **1** with NaOCl as a terminal oxidant was followed by a Wittig reaction with phosphorus ylide **2** to give the α,β-unsaturated ester **3**. Subsequent saponification led to the corresponding acid **4**, which served as substrate for a ruthenium-catalyzed diastereoselective hydrogenation using a Mandyphos-derived catalyst system to set the second stereogenic center. Esterification of the resulting (2*R*,4*S*)-amino ester **5** with concomitant deprotection finally gave amino ester **6** (Scheme 1).

Due to the anticipated large production volumes of LCZ696, the need for an improved manufacturing process of sacubitril was identified early on during development. Efforts focused on key intermediate **6**, as this intermediate combines—with the exception of the succinyl moiety—all essential structural and functional elements of sacubitril, in particular, both stereogenic centers, the aromatic biphenyl moiety as well as the amino and ester functionalities. Following the in-depth evaluation of various synthetic strategies, assembly of key intermediate **6** from itaconic acid monomethyl ester (**7**) and biphenylacetic acid (**10**) was identified as the preferred option (Scheme 2).[6]

The chosen strategy allows for (i) a late installation of the amino functionality, reducing the synthetic challenges due to the presence of only carbon, hydrogen, and oxygen, (ii) the avoidance of any protecting groups in the synthesis, and (iii) a fast buildup of structural complexity from structurally simple building blocks.

RESULTS AND DISCUSSION

Introduction of the first chiral center was efficiently achieved by an asymmetric hydrogenation of readily available itaconic acid monomethyl ester (**7**).[7] As the transformation has been widely used to benchmark new chiral ligands for hydrogenation reactions, ample literature precedent was available for the specific transformation.[8] Screening of reaction conditions focused on the identification of a high-performing catalyst system that provided the chiral acid **9** in high yield and excellent purity as a single enantiomer. Low catalyst loadings in an environmentally benign reaction solvent were targeted, and process conditions should be compatible with standard commercial hydrogenation equipment. The (*R*,*R*)-Ph-BPE-derived rhodium complex **8**[9] in methanol as reaction solvent at 30 °C and a hydrogen pressure of 10 bar proved effective to provide the best performance among the catalyst systems screened. Under these conditions, complete conversion to (*R*)-methyl succinic acid monomethyl ester (**9**) was observed, providing the product in high purity and excellent enantioselectivity (Table 1, all entries).

While higher hydrogen pressure slightly increased the reaction rate, the overall reaction performance (i.e., yield and quality) was found to be insensitive to the applied pressure (entries 1, 4, and 5). The reaction performed well even at moderate reaction temperatures, with lower temperatures generally leading to improved product quality due to reduced levels of substrate and product decomposition, while still maintaining an adequate reaction rate (entries 1−3). The reaction concentration was determined to have a positive impact on the reaction rate and a moderately beneficial impact on product quality. Concentrations as high as 1.30 g/mL could be readily applied, greatly improving the productivity of the reaction (entries 1, 7, and 8). Catalyst loadings as low as S/C 74000:1 were successfully tested without a noticeable impact on product quality and enantiopurity (entry 6).

Neat (*R*)-methyl succinic acid monomethyl ester (**9**) is an oil under ambient conditions.[10] As a consequence of its physical properties and due to the high purity of the product, (*R*)-methyl succinic acid monomethyl ester (**9**) was used without further

Scheme 1. Established Synthesis of Key Intermediate 6

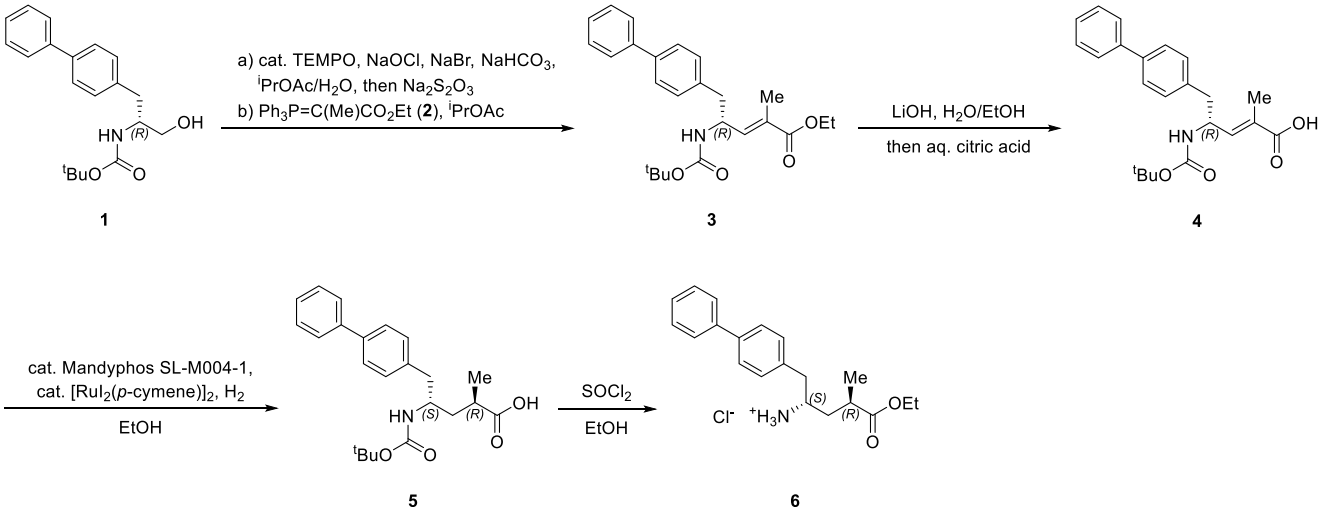

https://dx.doi.org/10.1021/acs.joc.0c00473
J. Org. Chem. XXXX, XXX, XXX−XXX

Scheme 2. New Synthesis of Key Intermediate 6

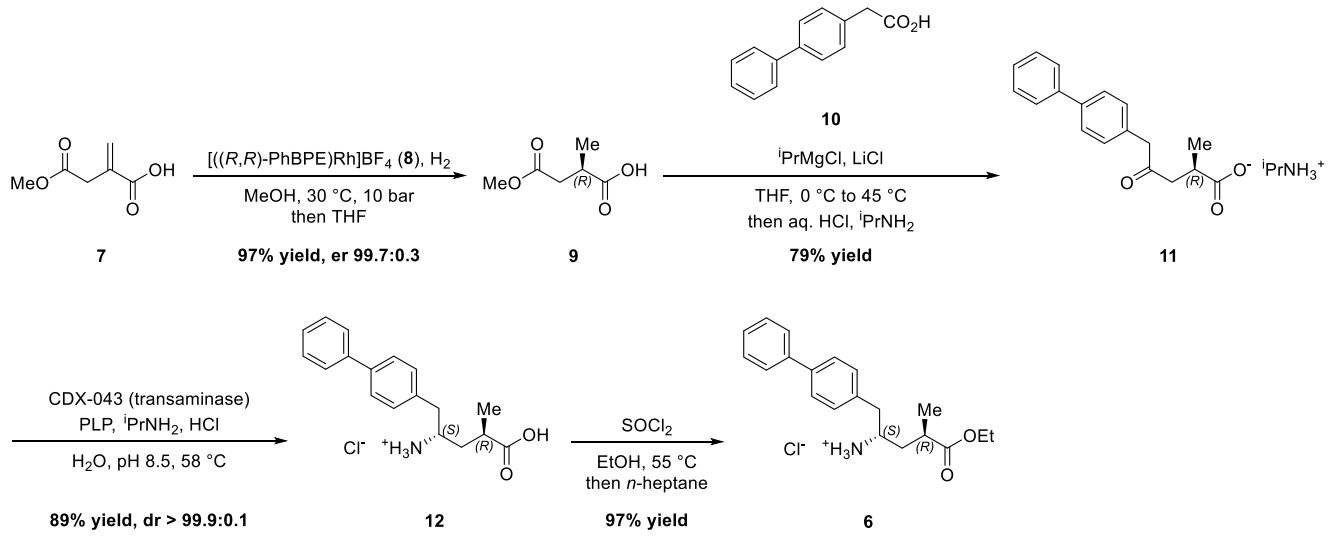

Table 1. Optimization of Reaction Conditions for Asymmetric Hydrogenation of Itaconic Acid Monomethyl Ester (7)[a]

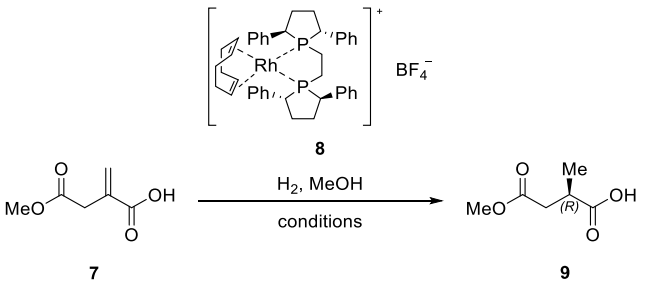

entry	pressure (bar)	catalyst loading (S/C)	conversion[b] (%)	purity[b] (%)	er[c]
1	10	35000:1	99.9	98.0	99.1:0.9
2[d]	10	35000:1	99.9	98.0	99.1:0.9
3[e]	10	35000:1	99.8	98.1	98.8:1.2
4	7	35000:1	>99.9	98.6	98.9:1.1
5	15	35000:1	>99.9	98.6	99.0:1.0
6	10	74000:1	99.8	98.5	98.4:1.6
7[f]	10	35000:1	>99.9	98.6	98.8:1.2
8[g]	10	35000:1	99.6	98.7	98.6:1.4

[a]All reactions were performed at multigram scale in a stainless steel hydrogenation reactor. Unless otherwise noted, all reactions were run at 30 °C and a concentration of 1.0 g/mL substrate for 19−23 h. [b]Determined by GC analysis after workup. [c]Determined by chiral GC analysis after workup. [d]Reaction performed at 20 °C; total reaction time 39 h. [e]Reaction performed at 35 °C. [f]Reaction performed at a concentration of 0.72 mL/g substrate. [g]Reaction performed at a concentration of 1.30 mL/g substrate.

purification in the next step. Workup and isolation consisted of a solvent exchange to THF, the reaction solvent used in the next step, with control of trace amounts of methanol to avoid interference with the use of basic Grignard reagent ^{i}PrMgCl. Small amounts of insolubles were removed by treatment with microcrystalline cellulose and subsequent filtration to provide (*R*)-methyl succinic acid monomethyl ester (**9**) as a concentrated solution.

The results of the process development on lab scale were fully confirmed on kilogram scale, overall exceeding the performance on lab scale likely due to reduced impact of incomplete inertization at larger reaction scale. Under typical reaction conditions using S/C 50000:1, (*R*)-methyl succinic acid monomethyl ester (**9**) was obtained in 97% yield (corrected for assay) and an enantiomeric ratio of 99.7:0.3.

The high concentration of the hydrogenation reaction in combination with the minimal stirring volume of the reactor inevitably results in large batch sizes. As a consequence, the specific surface area available to remove the released reaction heat of the exothermic hydrogenation reaction is small compared to lab-scale reactions. In order to gain additional process understanding and further improve the control of the heat release rate, a series of calorimetric (RC1) experiments were performed to investigate the impact of stirring speed and pressure on the heat release rate. When changing the stirring speed from 640 to 100 rpm over 3 min at constant hydrogen pressure, a significant decrease of the heat flow with subsequent stabilization at lower level was observed (see Figure S11). Concomitantly, the internal temperature of the reaction decreased, while the jacket temperature, due to the reduced heat flow, increased.[11] A similar behavior was observed for a reduction of the pressure from 8 to 5 bar over 2 min at constant stirring speed (see Figure S12). Overall, the results of the series of RC1 experiments allowed us to define suitable parameters for stirring speed and pressure on production scale, in particular during the initiation phase of the reaction.

During initial process development on lab scale, inconsistent results for the enantiomeric purity of (*R*)-methyl succinic acid monomethyl ester (**9**) were observed, in particular for reactions run at low catalyst loadings. Control experiments showed significant conversion in the absence of the chiral catalyst, leading to formation of racemic product *rac*-**9** in up to 20% conversion overnight. As no background reactivity was observed in glass-lined equipment with PTFE-coated magnetic stirrers, a potential catalytic activity of stainless steel as the material of construction was investigated. No negative impact on enantiopurity was observed when stainless steel powder with a high surface area was spiked to reactions in glass-lined equipment. In addition, reactions run in a previously unused stainless steel hydrogenation reactor led to product formation in high enantiopurity. The focus of the investigations was therefore shifted to the presence of trace impurities that could not be

https://dx.doi.org/10.1021/acs.joc.0c00473
J. Org. Chem. XXXX, XXX, XXX−XXX

Scheme 3. Synthesis of γ-Keto Acid 16 via Ivanov Reaction of Ester 7 and Biphenylacetic Acid (10) Using a Flow Reactor[a]

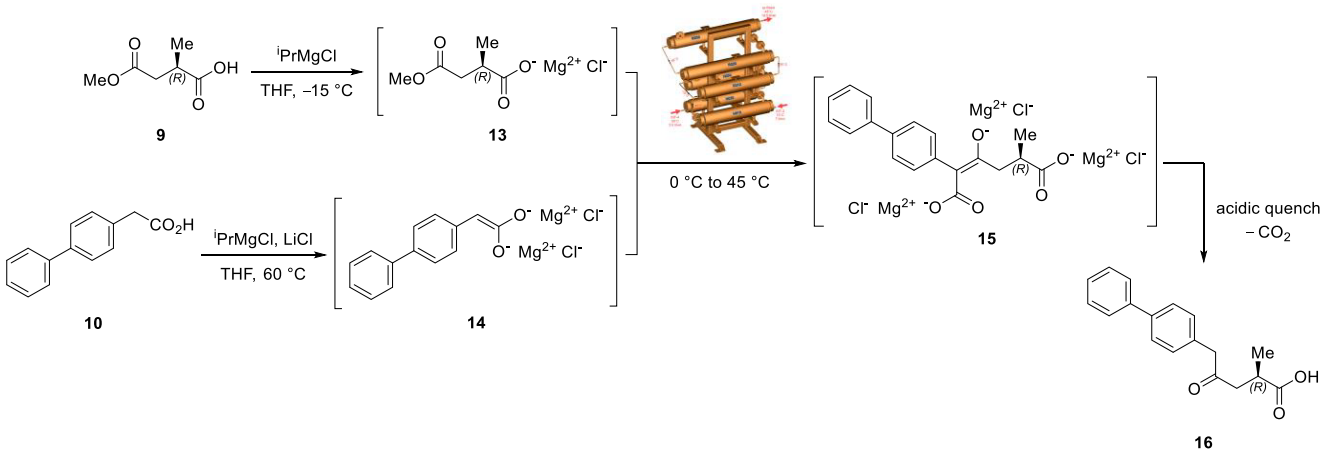

[a]Compounds in brackets represent nonisolated reaction intermediates.

removed with standard cleaning procedures in place.[12] Complete suppression of background reactivity could finally be achieved in stainless steel equipment by applying a wash with an aqueous cysteine solution at basic pH value.[13]

The presence of residual chloride anions in itaconic acid monomethyl ester (**7**) was found to negatively affect the reaction rate.[14] While affected reactions did achieve complete conversion, and the enantiomeric purity of the product (*R*)-methyl succinic acid monomethyl ester (**9**) remained high, low ppm levels of chloride prolonged reaction times until the required conversion was achieved. The impact of residual chloride on the reaction rate could be successfully reproduced in a spiking experiment with Bu_4NCl. Chloride is assumed to affect the catalytically active species, either by coordination to the cationic rhodium catalyst, thereby competing with the substrate and reducing the amount of active catalyst available in the system, or by formation of catalytically less active complexes.[15] Modifications in the manufacturing process in combination with control of residual chloride in itaconic acid monomethyl ester (**7**) as a safeguard allowed us to efficiently mitigate the negative impact of residual chloride and ensure consistent performance of the hydrogenation reaction.

Assembly of γ-ketoacid **16** relied on an Ivanov reaction between ester **9** and biphenylacetic acid (**10**) (Scheme 3).[16] The carboxylic acid moiety of (*R*)-methyl succinic acid monomethyl ester (**9**) was converted *in situ* to the corresponding electrophilic carboxylate salt **13** at −15 °C prior to reaction with nucleophilic dianion **14**, formed by deprotonation of biphenylacetic acid (**10**) with ^{i}PrMgCl in the presence of LiCl at 60 °C. Excess Grignard reagent had to be employed to achieve deprotonation of the initially formed β-ketocarboxylate to the corresponding β-ketoenol carboxylate **15**. Under inert conditions, dianion **14** was found to be stable at 60 °C over prolonged time without loss of reactivity. The use of the carboxylate salt **13** as substrate in the Ivanov reaction allowed us to efficiently differentiate the reactivity of the two carbonyl groups in compound **13**, while preventing epimerization of the stereogenic center under the basic reaction conditions.[17] Upon acidic quench, decarboxylation of the intermediately formed β-ketoenol carboxylate **15** occurred, leading to formation of the desired γ-ketoacid **16**.

While the Ivanov reaction performed well on small scale (as semibatch process), significantly decreased performance was observed on larger scale. With increasing reaction scale, short addition times and efficient temperature control in the exothermic Ivanov reaction were challenging to achieve, resulting in the formation of various byproducts and incomplete conversion. The decreased performance could easily be rationalized by the simultaneous presence of multiple anionic species (e.g., β-ketoenol carboxylate **15** and dianion **14**) in the same reaction volume at the same time. These anionic species could either act as nucleophiles or bases. Analysis of the impurity profile showed that the byproducts were mainly associated with the instability of the β-ketoenol carboxylate **15** under the reaction conditions of the batch process, leading to over-reaction of the corresponding decomposition products with dianion **14** or quench of dianion **14** by protonation. As a consequence, separation of the multiple anionic species by time and space using a flow reactor to perform the Ivanov reaction was investigated and successfully implemented. In the optimized setup, the solutions containing carboxylate salt **13** and dianion **14** were separately prepared in batch reactors, then brought together using a flow reactor, followed by addition of the product stream leaving the flow reactor to a quench solution in semibatch mode again.

The flow reaction was optimized in depth combining batch and flow experiments at lab and kilolab scale, relying largely on a design-of-experiment (DoE) approach. In addition, extensive use was made of computational simulations to predict and understand aspects that were experimentally challenging to investigate, e.g., mixing behavior or temperature profiles along the flow reactor. The temperature profile and the reaction time in the flow reactor were found to possess a significant impact on the outcome of the reaction, requiring fine-tuning to optimize conversion and product quality. Analysis of the conversion indicated that about 75% of the overall product formation occurred within the first seconds after mixing of carboxylate salt **13** and dianion **14**. While mixing was best performed at low temperature to achieve the desired product quality, a higher temperature level was subsequently needed to maximize conversion. As a consequence, a two-stage temperature profile was implemented, with a first stage at 0 °C and a residence time of 10−20 s, followed by a second stage at 45 °C with a residence time of 160−220 s.

During process development, dianion **14** was identified to form metastable solutions at temperatures below 55 °C, leading to crystallization upon induction, e.g. by addition of seed

https://dx.doi.org/10.1021/acs.joc.0c00473
J. Org. Chem. XXXX, XXX, XXX−XXX

crystals. The crystal structure of dianion **14** could be experimentally confirmed, showing two moieties of dianion **14** that coordinate to four magnesium cations. The magnesium cations are bridged by chloride ions, and the empty coordination spaces are occupied by THF molecules (see Figure S1).[18,19] The planes of the enolate functionalities of the two moieties of dianion **14** are oriented in a perpendicular fashion to each other.

Due to the metastability of solutions of dianion **14** in THF, the feedstream of dianion **14** had to be kept at 60 °C. The correct mixing temperature for the two feedstreams at the point of mixing was consequently achieved by lowering the temperature of the feedstream for carboxylate salt **13**. The stoichiometry between carboxylate salt **13** and dianion **14** was identified as a key reaction parameter to achieve consistently high product quality. With the feedstreams possessing defined concentrations, adjustment of the stoichiometry could be conveniently achieved by adjustment and control within a narrow range of the flow rates of both feedstreams. The nature of the base showed a pronounced effect on the reaction performance, with ^{i}PrMgCl providing superior results.[20] Furthermore, lithium was found to positively influence conversion in the flow reaction, even when present in substoichiometric amounts.

The outcome of the process development formed the basis for the *in silico* design of the flow reactor. While the reaction could be tested on kilogram scale in available multipurpose flow equipment (see the Supporting Information for details), a suitable reactor had to be designed and built from scratch for larger production scales based on the results from process development on lab scale, verification runs on kilogram scale, and software simulations. The requirement to be "right first time" as a result of limited options for modification of the reactor after construction was successfully met, with the performance characteristics of the newly designed reactor closely matching the predictions.[21]

The process stream from the flow reactor was immediately quenched by addition to water upon leaving the flow reactor. Upon collection of a defined volume of process stream, workup, crystallization, and isolation of γ-ketoacid **16** continued in a batch mode. Under the final process conditions, acidification of the quenched reaction mixture with aqueous hydrochloric acid led to concomitant decarboxylation of β-ketoenol carboxylate **15**. The rate of gas evolution could be controlled by the addition speed of aqueous hydrochloric acid. Subsequent phase separation and washing of the organic phase with NaCl solution to remove residual salts and excess acid provided a solution of γ-ketoacid **16** in THF.

Unconverted biphenylacetic acid (**10**), present due to its use in excess in the Ivanov reaction and its generation upon quench of the dianion **14**, constituted the major impurity in γ-ketoacid **16**. General quality considerations and an inhibitory effect of biphenylacetic acid (**10**) in the subsequent transamination reaction required its efficient removal during workup and crystallization.[22] While initial attempts to isolate the free γ-ketoacid **16** failed to meet both quality and yield targets at the same time, the investigation of various amines as salt forming agents proved to be more successful, allowing isolation of γ-ketoacid **16** as the corresponding ammonium salts in high yield and purity. Formation of an ammonium salt provided the additional benefit to isolate γ-ketoacid **16** directly from THF, thus avoiding the use of additional organic solvents.

The choice of amine for salt formation was mainly driven by process considerations, in particular to ensure compatibility with the subsequent transamination step. Serendipitously, isopropylamine, used as amine donor in the subsequent transamination reaction, was among the best performing amines screened, providing optimum results with respect to both depletion of biphenylacetic acid (**10**) and isolated yield of γ-ketoacid **16**. Subsequent process development emphasized process robustness to achieve consistency in yield of isopropylammonium salt **11** and levels of residual biphenylacetic acid (**10**) across a broad range of input qualities of crude γ-ketoacid **16**. Design-of-experiment (DoE) studies proved to be valuable for the identification of optimal settings for key process parameters like the stoichiometry of the salt-forming agent ^{i}PrNH$_2$, the volume of THF, and the water content during crystallization. As low water content was found to positively impact the crystallization yield, the solution of γ-ketoacid **16** in THF was dried by azeotropic distillation. Addition of ^{i}PrNH$_2$ then led to isolation of γ-ketoacid **16** as the corresponding isopropylammonium salt **11**.

Scale-up of the process to kilogram scale occurred without challenges, confirming in particular the depletion of residual biphenylacetic acid (**10**) as well as the projected isolated yield of γ-ketoacid **11**. Under typical reaction conditions, γ-ketoacid **11** was obtained in 79% yield with a level of only 1.1% residual biphenylacetic acid (**10**). The stereogenic center proved to be stable under the reaction conditions, without any sign of racemization occurring under the reaction conditions, providing γ-ketoacid **11** as an enantiomerically pure compound.

Transformation of γ-ketoacid **11** to the corresponding (2*S*,4*R*)-amino acid **12** was enabled by a biocatalytic enzymatic transamination using CDX-043, a highly evolved *S*-selective transaminase (E.C. 2.6.1) obtained by directed enzyme evolution over multiple evolution rounds,[6b,23−25] with pyridoxal 5′-phosphate (PLP, vitamin B$_6$) as cofactor and isopropylamine[26] as amine donor. Due to the low solubility of both substrate **11** and product **12** in aqueous conditions, the reaction was run as a slurry-to-slurry process, remaining heterogeneous throughout the whole reaction time. Use of cosolvents (e.g., DMSO) or surfactants to improve mass transfer did not have a pronounced effect on reaction rate while generally negatively affecting enzymatic activity.

Transaminase CDX-043 had been optimized for increased thermal stability, which allowed to increase the reaction temperature to 58 °C without noticeable decrease of enzymatic activity over time to achieve low enzyme loadings. Optimum enzymatic activity was observed at pH 8.5, with the enzyme tolerating a wider pH range (pH 8.0−8.6) around the set point pH 8.5 without significant drop of activity. As variation of the pH value during the reaction was found to be minimal, initial adjustment of the pH value with isopropylamine and aqueous hydrochloric acid before addition of the enzyme was demonstrated to be sufficient, and the reaction was finally run in water in the absence of a buffer system.[27]

Enzymatic transamination reactions are reversible and as such establish an equilibrium between substrate and product that typically favors the ketone substrate over the amine product.[6] High conversion to the amine therefore requires to actively shift the equilibrium. In the case of enzymes accepting isopropylamine as an amine donor, this is generally achieved by either the use of a large excess of the amine donor isopropylamine or by applying slight vacuum to remove the volatile byproduct acetone from the reaction mixture.[6,28] In the present case, however, the reaction showed a pronounced preference for the amino acid product **12**, leading to typically 95% conversion with only

https://dx.doi.org/10.1021/acs.joc.0c00473
J. Org. Chem. XXXX, XXX, XXX−XXX

moderate excess of isopropylamine under atmospheric pressure, i.e., without concomitant removal of acetone.[29]

During early stages of process development, direct isolation of the free amino acid from the reaction mixture was envisioned, as the compound showed low solubility in aqueous media. While feasibility of the approach could be demonstrated, attempts to optimize the physical properties of the free amino acid in order to provide satisfactory filtration performance were met with limited success. The corresponding hydrochloride salt **12** was found to exhibit superior properties and offered the additional benefit of an aqueous workup due to its high solubility in aqueous 2-methyltetrahydrofuran (2-MeTHF).[30] Though alternative salt forming agents were expected to provide similar performance, the hydrochloride salt eliminated the risk to form mixtures of different salts in the next process step to amino ester **6**, and hydrochloric acid was therefore identified as the salt forming agent of choice. Under the optimized process conditions, the reaction mixture was acidified by addition of hydrochloric acid after completion of the transamination reaction, and the aqueous layer was extracted with 2-MeTHF. The denatured enzyme remained suspended in the aqueous layer and could be readily removed by phase separation. Trace amounts of residual enzyme were removed from the organic layer by treatment with activated charcoal. Following partial removal of 2-MeTHF under concomitant azeotropic water removal and subsequent addition of methyl *tert*-butylether (MTBE) as antisolvent, the amino acid hydrochloride **12** crystallized from solution and was isolated by filtration.

The robustness of the biocatalytic transamination was demonstrated on kilogram scale, providing highly pure amino acid **12** in approximately 90% yield as a single diastereoisomer. Compared to lab scale trials, reaction times for low enzyme loadings were generally shorter on kilogram scale, presumably as a result of improved mixing of the heterogeneous reaction mixture on larger scale. The typical levels of residual biphenylacetic acid (**10**) present in γ-ketoacid **11** did not negatively affect the reaction rate.

The transamination reaction highlights the significant benefits offered by biocatalytic transformations on scale: (i) products are generally obtained in high yields and excellent purity; (ii) biocatalytic transformations usually provide products with high stereoselectivities; (iii) mild reaction conditions are applied; (iv) reaction conditions are environmentally benign and possess limited thermal safety hazards; and (v) processes are typically operationally simple.

Esterification of γ-amino acid **12** to the corresponding ethyl ester **6** was performed in analogy to the previously established conditions using thionyl chloride in ethanol at 50 °C.[5] Upon complete conversion, typically reached within 1 h, a solvent exchange from ethanol to *n*-heptane induced crystallization, providing ethyl ester **6** in high yield and excellent HPLC purity. The results from process development on lab scale were successfully confirmed on kilogram scale, with the product **6** isolated in typically 97% yield and high purity as a single diastereoisomer.

Reduction of the overall environmental footprint associated with the synthesis of sacubitril was a major incentive for the development of the new manufacturing process. Due to the anticipated large production volumes of LCZ696, reduced resource consumption results in a significant positive impact on the environmental sustainability. The established and new manufacturing processes were compared on the basis of the total carbon dioxide release (TCR),[31] with sacubitril calcium as the reference (Figure 2). The associated process mass intensity (PMI) values are listed in Table 2.

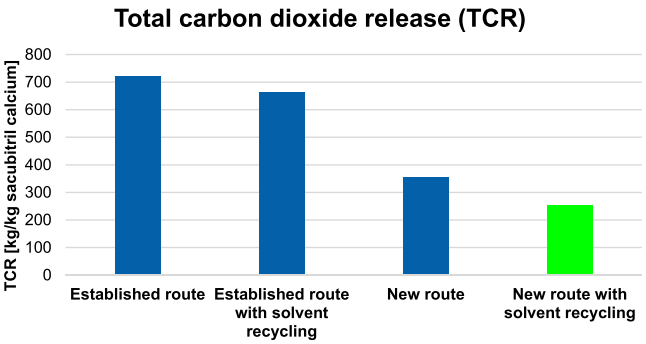

Figure 2. Improvement in environmental sustainability based on total carbon dioxide release.

Table 2. Process Mass Intensity Values for Established and New Routes[a]

route	cumulative PMI (kg/kg product)	cumulative organics PMI (kg/kg product)	cumulative aqueous PMI (kg/kg product)
established route	437	267	170
established route[b]	411	242	170
new route	211	132	80
new route[b]	167	88	80

[a]All PMI values are given per kilogram of sacubitril calcium as the reference. [b]Including solvent recovery.

While the shortening of the synthetic route, from 10 chemical transformations for the established route to only 5 for the new route, clearly represents the major contribution,[32] rigorous implementation of solvent recycling for the reaction solvents THF, 2-MeTHF and *n*-heptane used at large volumes for commercial production allowed us to leverage further reduction potential. Overall, approximately a 3-fold reduction of the TCR could be achieved by introduction of the new manufacturing process.

CONCLUSION

In summary, a new synthetic route to compound **6**, a key intermediate in the manufacture of sacubitril, one of the active components in LCZ696, was developed and successfully implemented on commercial production scale. The design of the synthesis relies on the strategic use of chemocatalysis, biocatalysis, and manufacture in flow as state-of-the-art technologies to meet current efficiency and sustainability requirements for pharmaceutical manufacturing processes.

EXPERIMENTAL SECTION

General Information. Transaminase CDX-043 was obtained from Codexis Inc., Redwood City, CA. All other materials, reagents, and solvents were purchased from commercial sources and used without further purification. NMR spectra were obtained on a Bruker Avance III 400 MHz spectrometer operating at 400 MHz for ^{1}H-measurements and 100 MHz for ^{13}C{^{1}H}-measurements. All spectra were recorded in DMSO-d_6. Chemical shifts (δ) are reported in ppm relative to the tetramethylsilane signal (0 ppm) or residual protio-solvent (2.50 ppm) for ^{1}H NMR spectra and relative to the solvent resonance (39.5 ppm) for ^{13}C{^{1}H}-NMR spectra. Infrared spectra were recorded on a Perkin Spectrum 100 spectrometer and are reported as wavenumbers with

https://dx.doi.org/10.1021/acs.joc.0c00473
J. Org. Chem. XXXX, XXX, XXX−XXX

units of reciprocal centimeters (cm^{-1}). High-resolution mass spectra (electrospray ionization, ESI or ESI-TOF) were measured on an LTQ Orbitrap XL or a Waters Xevo G2-XS QTof mass spectrometer. The enantiomeric purity of compound **9** was measured on an Agilent HPLC 1200, equipped with a Daicel Chiralpak column (AY-3, 150 mm × 4.6 mm × 3.0 μm). Melting points were measured on a Mettler-Toledo MP90 and are uncorrected. Details on the flow reactor setup are presented in the Supporting Information.

Compound 9. Compound **7** (5.0 kg, 34.4 mol, 1.0 equiv) and MeOH (4.0 kg, degassed with nitrogen) were charged to an autoclave at IT = 20 °C, followed by addition of a solution of [((*R*,*R*)-Ph-BPE)Rh]BF_4 (470 mg, 0.6 mmol, S/C = 57000:1) in MeOH (50.0 g, degassed with nitrogen) under nitrogen atmosphere. The hydrogenation vessel was flushed with hydrogen three times and pressurized to 10 bar (gauge) subsequently. The reaction mixture was warmed to IT = 30 °C and stirred for 10 h. Hydrogen was exchanged with nitrogen, and the reaction mixture was cooled to IT = 20 °C and diluted with THF (4.5 kg). The solvent was evaporated at JT = 40 °C *in vacuo*. The residue was twice taken up in THF (4.5 kg) and subsequently concentrated to give compound **9** as a yellow oil (4.9 kg, 33.5 mol, yield 97%; assay 84% (w/w), yield corrected for assay), containing residual THF. Compound **9** was used in the next step without further purification.

^{1}H NMR (DMSO-d_6, 400 MHz): δ 12.21 (s, 1 H), 3.57 (s, 3 H), 2.78−2.63 (m, 1 H), 2.56 (dd, J = 8.0, 16.4, 1 H), 2.39 (dd, J = 5.6, 16.8, 1 H), 1.10 (d, J = 7.2, 3 H) (signals of residual THF at δ 3.60 and 1.76 disregarded). ^{13}C{^{1}H}-NMR (DMSO-d_6, 100 MHz): δ 176.6, 172.4, 51.6, 37.2, 35.6, 17.1 (signals of residual THF at δ 67.4 and 25.5 disregarded). IR (ATR) ν 2976, 2887, 1731, 1701, 1218, 1182, 817, 730, 682 cm^{-1}. HRMS (ESI) m/z: [M + H]$^+$ calcd for $C_6H_{11}O_4$ 147.0652, found 147.0652. HPLC (Daicel Chiralpak AY-3, 0.1% acetic acid in heptane:2-propanol 90:10, flow rate 1.0 mL/min, λ = 210 nm, T = 30 °C, t_{major} = 6.2 min, t_{minor} = 4.9 min, er = 99.7:0.3; see the Supporting Information for sample preparation).

Compound 11. Compound **9** (2.2 kg, 15.1 mol, 1.0 equiv) and THF (12.0 kg) were charged to a reactor, followed by inertization with nitrogen. The solution was cooled to IT = 0 °C, and then ^{i}PrMgCl solution in THF (20.9% (m/m), 7.8 kg, 15.9 mol, 1.1 equiv) was added at IT = 0 °C. The reaction mixture was heated to IT = 35 °C, stirred for 1 h, then cooled to IT = 20 °C. The resultant solution was filtered to afford a solution of compound **13** in THF.

Compound **10** (3.5 kg, 16.3 mol, 1.1 equiv), LiCl (0.7 kg, 17.2 mol, 1.1 equiv), and THF (19.3 kg) were charged to a reactor, followed by inertization with nitrogen. The solution was warmed to IT = 45 °C, then ^{i}PrMgCl solution in THF (20.9% (m/m), 24.6 kg, 50.0 mol, 3.3 equiv) was added at IT ≤ 45 °C. The reaction mixture was heated to IT = 60 °C and stirred for 2 h. The resultant solution was filtered to afford a solution of intermediate **14** in THF.

The THF solution of compound **13** was pumped through precooling loops at JT = −15 °C with a flow rate of 56.1 g/min, while the THF solution of compound **14** was pumped through preheating loops at JT = 60 °C with a flow rate of 109.7 g/min. The two feedstreams were mixed in a T-mixer and then subsequently flowed through reactor loops at JT = 0 °C (residence time 12 s) and JT = 45 °C (residence time 170 s) and a back-pressure regulator set to ca. 5 bar(g). The reaction mixture was collected in a quench reactor preloaded with water (10.6 kg) at IT = 20 °C. After completion of the reaction, aqueous HCl solution (31%, 7.6 kg) was added slowly to adjust the pH value to pH 2.0. The phases were separated, and the organic layer was washed sequentially with aqueous sodium chloride solution (10% for first wash, 20% for second wash; 28.0 kg each). The resultant organic layer was evaporated *in vacuo*, and then fresh THF (50.0 kg) was added. Aqueous isopropylamine (70%, 2.2 kg, 1.7 equiv with respect to compound **16**) was slowly added at IT = 25 °C, leading to precipitation of compound **11**. The suspension was cooled to IT = 0 °C, and the solids were filtered off. The filter cake was washed with cold THF, and the solids were dried under vacuum to afford compound **11** as a white solid (3.9 kg, 11.9 mol, yield 79%). Mp = 163 °C. ^{1}H NMR (DMSO-d_6, 400 MHz): δ 7.67−7.62 (m, 2 H), 7.59 (d, J = 8.2, 2 H), 7.45 (dd, J = 6.9, 8.4, 2 H), 7.39−7.31 (m, 1 H), 7.30−7.22 (m, 2 H), 3.80 (s, 2 H), 3.12 (m, J = 6.4, 1 H), 2.81 (dd, J = 7.8, 16.4, 1 H), 2.57 (dt, J = 6.3, 7.5, 1 H), 2.34 (dd, J = 6.2, 16.3, 1 H), 1.09 (d, J = 6.4, 6 H), 0.99 (d, J = 7.1, 3 H). ^{13}C{^{1}H}-NMR (DMSO-d_6, 100 MHz): δ 206.5, 178.0, 140.0, 138.3, 134.4, 130.3, 129.5, 128.9, 127.3, 126.5, 48.6, 46.3, 42.3, 36.6, 22.1, 17.8. IR (ATR) ν 2977, 2880, 1716, 1538, 1405, 1394, 763, 736 626 cm^{-1}. HRMS (ESI, excluding isopropylammonium counterion) m/z: [M + Na]$^+$ calcd for $C_{18}H_{18}NaO_3$ 305.1154, found 305.1162.

Compound 12. Water (17.7 kg) and aqueous HCl (31%, 3.5 kg) were charged to a reactor, followed by sequential addition of compound **11** (4.4 kg, 12.9 mol, 1.0 equiv) and PLP (36 g, 146 mmol, 0.01 equiv). The resultant suspension was heated to IT = 58 °C, and the pH value was adjusted to pH 8.5 with aqueous isopropylamine (70%, ca. 2.8 kg). A suspension of transaminase CDX-043 (73.0 g) in water (0.4 kg) was added to the reaction mixture, and stirring was continued at IT = 58 °C for 20 h. The reaction mixture was cooled to IT = 25 °C, 2-MeTHF (25.0 kg) was added, and the pH value was adjusted to pH 2.0 by addition of aqueous HCl (31%, ca. 1.9 kg), followed by addition of solid NaCl (3.7 kg). The resultant biphasic mixture underwent phase separation, and the aqueous layer was extracted with 2-MeTHF (2 × 12.5 kg). The organic layers were combined and washed with aqueous NaCl solution (10%, 9.8 kg). Active carbon (180.0 g) was added, followed by stirring at room temperature for 30 min. The solids were filtered off, and the filtrate was concentrated *in vacuo* to remove water azeotropically, leading to partial crystallization of compound **12**. MTBE (26.9 kg) was added slowly to the resulting suspension at IT = 40 °C to complete crystallization. The suspension was cooled to IT = 20 °C, and the solids were filtered to afford compound **12** as a white solid (3.6 kg, 11.3 mol, yield 89%). Mp = 208 °C. ^{1}H NMR (400 MHz, DMSO-d_6): δ 12.27 (s, 1 H), 8.29 (s, 3 H), 7.65 (ddd, J = 1.6, 7.7, 10.9, 4 H), 7.46 (dd, J = 7.0, 8.4, 2 H), 7.36 (dd, J = 2.2, 7.9, 3 H), 3.41 (dt, J = 3.9, 7.8, 2 H), 3.08 (dd, J = 5.6, 13.8, 1 H), 2.85 (dd, J = 7.7, 13.8, 1 H), 2.74−2.60 (m, 1 H), 1.85 (ddd, J = 5.3, 8.8, 14.1, 1 H), 1.60 (ddd, J = 5.7, 7.9, 14.0, 1 H), 1.06 (d, J = 7.0, 3 H). ^{13}C{^{1}H}-NMR (100 MHz, DMSO-d_6): δ 177.0, 140.3, 139.1, 136.1, 130.5, 129.4, 127.9, 127.3, 127.0, 50.8, 38.6, 36.2, 35.4, 18.0; IR (ATR) ν 2855, 1692, 1680, 1485, 1219, 1183, 752, 729, 682 cm^{-1}. HRMS (ESI, excluding isopropylammonium counterion) m/z: [M + H]$^+$ calcd for $C_{18}H_{22}NO_2$ 284.1645, found 284.1667.

Compound 6. Compound **12** (3.5 kg, 10.9 mol, 1.0 equiv) and ethanol (19.0 kg) were charged to a reactor. The resulting suspension was warmed to IT = 40 °C, and then $SOCl_2$ (1.3 kg, 10.9 mol, 1.0 equiv) was added dropwise at IT = 40 °C. Upon completion of the addition, the reaction mixture was warmed to IT = 50 °C and stirred for 0.5 h. The reaction mixture was concentrated *in vacuo* to remove ethanol, and then *n*-heptane (17.5 kg) was added. The resulting suspension was further concentrated *in vacuo*, and the distilled solvent was replenished by fresh *n*-heptane (ca. 7.0 kg). The suspension was heated to IT = 65 °C to give a clear solution, followed by subsequent slow cooling to IT = 10 °C. The solids were filtered, and the filter cake was washed with a precooled mixture of ethanol and *n*-heptane (5.0 kg, 5:95 (m/m)) and dried to afford compound **6** as a white solid (3.7 kg, 10.6 mol, yield 97%). Mp = 161 °C. ^{1}H NMR (400 MHz, DMSO-d_6): δ 8.22 (s, 3 H), 7.77−7.56 (m, 4 H), 7.46 (dd, J = 6.9, 8.4, 2 H), 7.40−7.32 (m, 3 H), 3.98 (q, J = 7.1, 2 H), 3.38 (s, 1 H), 3.06 (dd, J = 5.4, 13.7, 1 H), 2.91−2.65 (m, 2 H), 2.00−1.76 (m, 1 H), 1.59 (s, 1 H), 1.18−0.96 (m, 6 H). ^{13}C{^{1}H}-NMR (100 MHz, DMSO-d_6) δ 175.2, 140.3, 139.1, 136.0, 130.5, 129.4, 127.9, 127.3, 127.0, 60.5, 50.9, 39.8, 39.6, 39.4, 38.6, 36.0, 35.5, 18.0, 14.4. IR (ATR) ν 2975, 2884, 1727, 1514, 1488, 1210, 1188, 1158, 758, 748, 731, 691 cm^{-1}. HRMS (ESI, excluding chloride counterion) m/z: [M + H]$^+$ calcd for [$C_{20}H_{26}NO_2$]$^+$ 312.2000, found 312.2008.

■ ASSOCIATED CONTENT

Supporting Information

The Supporting Information is available free of charge at https://pubs.acs.org/doi/10.1021/acs.joc.0c00473.

X-ray data for compound **14** (CIF)

NMR spectra (for compounds **9**, **11**, **12** and **6**), HPLC data for compound **9**, RC1 data for hydrogenation

https://dx.doi.org/10.1021/acs.joc.0c00473
J. Org. Chem. XXXX, XXX, XXX−XXX

reaction, and details on equipment for flow reaction (PDF)

AUTHOR INFORMATION

Corresponding Author

Florian Kleinbeck − *Chemical & Analytical Development, Novartis Pharma AG, 4056 Basel, Switzerland;* orcid.org/0000-0002-2705-4629; Email: florian.kleinbeck@novartis.com

Authors

Xingxian Gu − *Suzhou Novartis Technical Development Co., Ltd., Changshu City, Jiangsu Province 215537, P.R. China*

Jibin Zhao − *Suzhou Novartis Technical Development Co., Ltd., Changshu City, Jiangsu Province 215537, P.R. China*

Like Chen − *Suzhou Novartis Technical Development Co., Ltd., Changshu City, Jiangsu Province 215537, P.R. China*

Yunzhong Li − *Suzhou Novartis Technical Development Co., Ltd., Changshu City, Jiangsu Province 215537, P.R. China*

Bo Yu − *Suzhou Novartis Technical Development Co., Ltd., Changshu City, Jiangsu Province 215537, P.R. China*

Xiangguang Tian − *Suzhou Novartis Technical Development Co., Ltd., Changshu City, Jiangsu Province 215537, P.R. China*

Zhongcheng Min − *Suzhou Novartis Technical Development Co., Ltd., Changshu City, Jiangsu Province 215537, P.R. China*

Su Xu − *Suzhou Novartis Technical Development Co., Ltd., Changshu City, Jiangsu Province 215537, P.R. China*

Huijuan Gu − *Suzhou Novartis Technical Development Co., Ltd., Changshu City, Jiangsu Province 215537, P.R. China*

Junjie Sun − *Suzhou Novartis Technical Development Co., Ltd., Changshu City, Jiangsu Province 215537, P.R. China*

Xiaoquan Lu − *Suzhou Novartis Technical Development Co., Ltd., Changshu City, Jiangsu Province 215537, P.R. China*

Meng Chang − *Suzhou Novartis Technical Development Co., Ltd., Changshu City, Jiangsu Province 215537, P.R. China*

Xufan Wang − *Suzhou Novartis Technical Development Co., Ltd., Changshu City, Jiangsu Province 215537, P.R. China*

Liqun Zhao − *Suzhou Novartis Technical Development Co., Ltd., Changshu City, Jiangsu Province 215537, P.R. China*

Shengqing Ye − *Suzhou Novartis Technical Development Co., Ltd., Changshu City, Jiangsu Province 215537, P.R. China*

Hongwei Yang − *Suzhou Novartis Technical Development Co., Ltd., Changshu City, Jiangsu Province 215537, P.R. China;* orcid.org/0000-0002-9136-5544

Yingtao Tian − *Suzhou Novartis Technical Development Co., Ltd., Changshu City, Jiangsu Province 215537, P.R. China*

Feng Gao − *Suzhou Novartis Technical Development Co., Ltd., Changshu City, Jiangsu Province 215537, P.R. China*

Yu Gai − *Suzhou Novartis Technical Development Co., Ltd., Changshu City, Jiangsu Province 215537, P.R. China*

Guanghua Jia − *Novartis Pharmaceuticals (China) Suzhou Operations, Riverside Industrial Park Changshu Economic Development Zone, Changshu, Jiangsu Province 215537, P.R. China*

Jingjing Wu − *Novartis Pharmaceuticals (China) Suzhou Operations, Riverside Industrial Park Changshu Economic Development Zone, Changshu, Jiangsu Province 215537, P.R. China*

Yan Wang − *Novartis Pharmaceuticals (China) Suzhou Operations, Riverside Industrial Park Changshu Economic Development Zone, Changshu, Jiangsu Province 215537, P.R. China*

Jianghua Zhang − *Novartis Pharmaceuticals (China) Suzhou Operations, Riverside Industrial Park Changshu Economic Development Zone, Changshu, Jiangsu Province 215537, P.R. China*

Xuesong Zhang − *Novartis Pharmaceuticals (China) Suzhou Operations, Riverside Industrial Park Changshu Economic Development Zone, Changshu, Jiangsu Province 215537, P.R. China*

Weichun Liu − *Novartis Pharmaceuticals (China) Suzhou Operations, Riverside Industrial Park Changshu Economic Development Zone, Changshu, Jiangsu Province 215537, P.R. China*

Xin Gu − *Novartis Pharmaceuticals (China) Suzhou Operations, Riverside Industrial Park Changshu Economic Development Zone, Changshu, Jiangsu Province 215537, P.R. China*

Xi Luo − *Novartis Pharmaceuticals (China) Suzhou Operations, Riverside Industrial Park Changshu Economic Development Zone, Changshu, Jiangsu Province 215537, P.R. China*

Hai Dong − *Novartis Pharmaceuticals (China) Suzhou Operations, Riverside Industrial Park Changshu Economic Development Zone, Changshu, Jiangsu Province 215537, P.R. China*

Huaimin Wang − *Novartis Pharmaceuticals (China) Suzhou Operations, Riverside Industrial Park Changshu Economic Development Zone, Changshu, Jiangsu Province 215537, P.R. China*

Berthold Schenkel − *Chemical & Analytical Development, Novartis Pharma AG, 4056 Basel, Switzerland*

Francesco Venturoni − *Chemical & Analytical Development, Novartis Pharma AG, 4056 Basel, Switzerland*

Paolo Filipponi − *Chemical & Analytical Development, Novartis Pharma AG, 4056 Basel, Switzerland;* orcid.org/0000-0002-8973-4339

Bertrand Guelat − *Chemical & Analytical Development, Novartis Pharma AG, 4056 Basel, Switzerland;* orcid.org/0000-0003-3872-4568

Thomas Allmendinger − *Chemical & Analytical Development, Novartis Pharma AG, 4056 Basel, Switzerland*

Bernhard Wietfeld − *Chemical & Analytical Development, Novartis Pharma AG, 4056 Basel, Switzerland*

Pascale Hoehn − *Chemical & Analytical Development, Novartis Pharma AG, 4056 Basel, Switzerland*

Nikola Kovacic − *Chemical & Analytical Development, Novartis Pharma AG, 4056 Basel, Switzerland*

Luca Hermann − *Chemical & Analytical Development, Novartis Pharma AG, 4056 Basel, Switzerland*

Thierry Schlama − *Chemical & Analytical Development, Novartis Pharma AG, 4056 Basel, Switzerland*

Thomas Ruch − *Chemical & Analytical Development, Novartis Pharma AG, 4056 Basel, Switzerland*

Nadine Derrien − *Pharmaceutical & Analytical Development, Novartis Pharma AG, 4056 Basel, Switzerland*

Philippe Piechon − *Novartis Institutes for Biomedical Research, Novartis Pharma AG, 4056 Basel, Switzerland*

Complete contact information is available at: https://pubs.acs.org/10.1021/acs.joc.0c00473

Author Contributions

The manuscript was written through contributions of all authors.

Notes

The authors declare no competing financial interest.

https://dx.doi.org/10.1021/acs.joc.0c00473
J. Org. Chem. XXXX, XXX, XXX−XXX

■ ACKNOWLEDGMENTS

We are indebted to Yvonne Richter, Dominique Bixel, Richard Kähny, Sibylle Müller, Sarah Monnerat, Barbara Bianchi, Marek Mahut, Markus Blatter, Angelique Nitsche, Evelyne Muller, Dorina Kotoni, Lorenzo Piccioni, Silke Schoenebeck, Roger Suremann, Corinne Marx, Ina Dix, and Trixie Wagner for support with experimental and analytical studies. We thank Andreas Seger, Lucy Browne, Damian Grainger, and Antonio Zanotti-Gerosa from Johnson Matthey, Scott Novick, Mandy Vink, and David Entwistle from Codexis, Inc., Esteban Rosasco and Alain Georg from Fluitec, as well as Viktor von Burg and Carlos Kreisel from Consolution AG for the fruitful and close collaborations. Radka Snajdrova and Elina Siirola are gratefully acknowledged for technical support and helpful discussions. We thank Ulrich Onken and Agnieszka Köttgen for the PMI and TCR calculations.

■ REFERENCES

(1) (a) Stewart, S.; MacIntyre, K.; Capewell, S.; McMurray, J. J. V. Heart failure and the aging population: an increasing burden in the 21st century? *Br. Heart J.* **2003**, *89*, 49−53. (b) Askoxylakis, V.; Thieke, C.; Pleger, S. T.; Most, P.; Tanner, J.; Lindel, K.; Katus, H. A.; Debus, J.; Bischof, M. Long-term survival of cancer patients compared to heart failure and stroke: A systematic review. *BMC Cancer* **2010**, *10*, 105−112. (c) Braunschweig, F.; Cowie, M. R.; Auricchio, A. What are the costs of heart failure? *Europace* **2011**, *13*, ii13−ii17. See also European Medicines Agency, Entresto Public Assessment Report, EMA/671279/2015.

(2) (a) McMurray, J. J. V.; Packer, M.; Desai, A. S.; Gong, J.; Lefkowitz, M. P.; Rizkala, A. R.; Rouleau, J. L.; Shi, V. C.; Solomon, S. D.; Swedberg, K.; Zile, M. R. Angiotensin-Neprilysin Inhibition versus Enalaprilin Heart Failure. *N. Engl. J. Med.* **2014**, *371*, 993−1004. (b) Sacks, C. A.; Jarcho, J. A.; Curfman, G. D. Paradigm Shifts in Heart-Failure Therapy - A Timeline. *N. Engl. J. Med.* **2014**, *371*, 989−991.

(3) Feng, L.; Karpinski, P. H.; Sutton, P.; Liu, Y.; Hook, D. F.; Hu, B.; Blacklock, T. J.; Fanwick, P. E.; Prashad, M.; Godtfredsen, S.; Ziltener, C. LCZ696: a dual-acting sodium supramolecular complex. *Tetrahedron Lett.* **2012**, *53*, 275−276.

(4) For an example, see: Beutler, U.; Boehm, M.; Fuenfschilling, P. C.; Heinz, T.; Mutz, J.-M.; Onken, U.; Mueller, M.; Zaugg, W. A High-Throughput Process for Valsartan. *Org. Process Res. Dev.* **2007**, *11*, 892−898.

(5) For the first synthesis of sacubitril, see: (a) Ksander, G. M.; Ghai, R. D.; deJesus, R.; Diefenbacher, C. G.; Yuan, A.; Berry, C.; Sakane, Y.; Trapani, A. Dicarboxylic Acid Dipeptide Neutral Endopeptidase Inhibitors. *J. Med. Chem.* **1995**, *38*, 1689−1700. (b) Hook, D.; Wietfeld, B.; Lotz, M. Process for Preparing Biaryl Substituted 4-Amino-Butyric Acid or Derivatives Thereof and their Use in the Production of NEP Inhibitors. WO 2008/031567 A1, March 20, 2008. (c) Zhu, G.; Ye, W.; Zheng, H.; Qian, L.; Wei, J.; Yang, L.; Li, Y.; Luo, L. New Process. WO 2014/032627 A1, March 06, 2014.

(6) (a) Kleinbeck-Riniker, F. K.; Martin, B.; Penn, G.; Venturoni, F.; Schlama, T.; Ruch, T.; Allmendinger, T.; Wietfeld, B., Filipponi, P. New Process and Intermediates. WO 2017/098430 A1, June 15, 2017. (b) Novick, S. J.; Dellas, N.; Alvizo, O.; Carcia, R. D.; Ching, C.; Entwistle, D. Engineered Transaminase Polypeptides for Industrial Biocatalysis. WO 2018/231462 A1 2018/231462 A1, December 20, 2018.

(7) Itaconic acid monomethyl ester is accessible from itaconic acid by acid-catalyzed selective monoesterification; see, e.g. (a) Devi, A. R.; Rajaram, S. An efficient and regiospecific esterification of dioic acids using PTSA. *Indian J. Chem.* **2000**, *39*, 294−296. (b) Ju, A.; Yan, Y.; Wang, D.; Luo, J.; Ge, M.; Li, M. A high molecular weight acrylonitrile copolymer prepared by mixed solvent polymerization: I. effect of monomer feed ratios on polymerization and stabilization. *RSC Adv.* **2014**, *4*, 64043−64052. Itaconic acid is commercially produced by fermentation for various industrial applications, e.g., as a co-monomer in polymerizations or as paint additive and is readily available on multi-ton scale at low cost.

(8) (a) Fürstner, A.; Bouchez, L. C.; Morency, L.; Funel, J.-A.; Liepins, V.; Porée, F.-H.; Gilmour, R.; Laurich, D.; Beaufils, F.; Tamiya, M. Total Syntheses of Amphidinolides B1, B4, G1, H1 and Structure Revision of Amphidinolide H2. *Chem. - Eur. J.* **2009**, *15*, 3983−4010. (b) Almena, J.; Monsees, A.; Kadyrov, R.; Riermeier, T. H.; Gotov, B.; Holz, J.; Börner, A. Highly Enantioselective Hydrogenation of Itaconic Acid Derivatives with a Chiral Bisphospholane-Rh(I) Catalyst. *Adv. Synth. Catal.* **2004**, *346*, 1263−1266. (c) Candy, M.; Tomas, L.; Parat, S.; Heran, V.; Bienaymé, H.; Pons, J.-M.; Bressy, C. A Convergent Approach to (−)-Callystatin A Based on Local Symmetry. *Chem. - Eur. J.* **2012**, *18*, 14267−14271. (d) van den Berg, M.; Minnaard, A. J.; Haak, R. M.; Leeman, M.; Schudde, E. P.; Meetsma, A.; Feringa, B. L.; de Vries, A. H. M.; Maljaars, C. E. P.; Willans, C. E.; Hyett, D.; Boogers, J. A. F.; Henderickx, H. J. W.; de Vries, J. G. Monodentate Phosphoramidites: A Breakthrough in Rhodium-Catalysed Asymmetric Hydrogenation of Olefins. *Adv. Synth. Catal.* **2003**, *345*, 308−322. (e) Zhu, S.-F.; Yu, Y.-B.; Li, S.; Wang, L.-X.; Zhou, Q. L. Enantioselective Hydrogenation of a-Substituted Acrylic Acids Catalyzed by Iridium Complexes with Chiral Spiro Aminophosphine Ligands. *Angew. Chem., Int. Ed.* **2012**, *51*, 8872−8875. (f) Zhang, W.; Zhang, X. Highly Enantioselective Hydrogenation of α-Dehydroamino Esters and Itaconates with Triphosphorous Bidentate Ligands and the Unprecedented Solvent Effect Thereof. *J. Org. Chem.* **2007**, *72*, 1020−1023. (g) Wu, S.; He, M.; Zhang, X. Synthesis of *ortho*-phenyl substituted MeO-BIPHEP ligand and its application in Rh-catalyzed asymmetric hydrogenation. *Tetrahedron: Asymmetry* **2004**, *15*, 2177−2180. (h) Kawano, H.; Ishii, Y.; Ikariya, T.; Saburi, M.; Yoshikawa, S.; Uchida, Y.; Kumobayashi, H. Ruthenium(II)-BINAP Complex Catalyzed Asymmetric Hydrogenation of Unsaturated Dicarboxylic Acids. *Tetrahedron Lett.* **1987**, *28*, 1905−1908.

(9) Pilkington, C. J.; Zanotti-Gerosa, A. Expanding the Family of Phospholane-Based Ligands: 1,2-Bis(2,5-diphenylphospholano)-ethane. *Org. Lett.* **2003**, *5*, 1273−1275.

(10) A boiling point of 108 °C at 0.5 mmHg has been reported for (*R*)-methyl succinic acid monomethyl ester **9**. See: Vazquez, M. L.; Mueller, R. A.; Talley, J. J.; Getman, D. P.; DeCrescenzo, G. A.; Sun, E. T. Alpha- and Beta-Amino Acid Hydroxyethylamino Sulfamic Acid Derivatives Useful as Retroviral Protease Inhibitors. US 6,156,768, December 05, 2000.

(11) The reaction was run in "T_R mode" in the RC1 equipment; i.e., the equipment kept the temperature of the reaction mixture constant.

(12) Standard cleaning protocols based on the use of nitric acid for removal of residual trace amounts of transition-metal catalysts from stainless steel hydrogenation equipment were not successful in suppressing the observed background reactivity.

(13) Complete removal of residual cysteine to avoid a negative impact on catalyst reactivity in subsequent batches could reliably be achieved by thorough rinsing with water.

(14) Inhibition of catalyst activity at levels comparable to chloride was similarly observed for other coordinating anions (e.g., carboxylic acids or sulfate).

(15) (a) Preetz, A.; Kohrt, C.; Meißner, A.; Wei, S.; Drexler, H.-J.; Buschmann, H.; Heller, D. Halide bridged trinuclear rhodium complexes and their inhibiting influence on catalysis. *Catal. Sci. Technol.* **2013**, *3*, 462−468. For a general review on halide effects in transition-metal catalysis, see: (b) Lautens, M.; Fagnou, K. Halide Effects in Transition Metal Catalysis. *Angew. Chem., Int. Ed.* **2002**, *41*, 26−47.

(16) (a) Ivanov, D.; Spassoff, A. Sur une méthode de préparation des acides phénylmalonique, ortho-chlorphénylmalonique et para-chlorphénylmalonique. *Bull. Soc. Chim. France* **1931**, *49*, 19. (b) Blagoev, B.; Ivanov, D. Syntheses with Polyfunctional Organomagnesium Compounds. *Synthesis* **1970**, *1970*, 615−627. For a general review on reactions of dianions of carboxylic acids and esters, see: (c) Petragnani, N.; Yonashiro, M. The Reactions of Dianions of Carboxylic Acids and Ester Enolates. *Synthesis* **1982**, *1982*, 521−578.

https://dx.doi.org/10.1021/acs.joc.0c00473
J. Org. Chem. XXXX, XXX, XXX−XXX

(17) Alternative substrates with differentiation of the two carbonyl functionalities (e.g., orthogonal diesters) were experimentally investigated but provided inferior results in the Ivanov reaction.
(18) It is interesting to note that crystallization was not observed in 2-methyltetrahydrofuran (2-MeTHF). This observation is in line with distinct differences in reactivity of dianion **14** compared to THF when prepared in 2-MeTHF as solvent.
(19) Coordination of the magnesium cations to the oxygen atoms of the dianion instead of the enolate carbon atom as observed in the X-ray crystal structure is in agreement with earlier reports from mechanistic and kinetic investigations of the Ivanov reaction. For details, see: Toullec, J.; Mladenova, M.; Gaudemar-Bardone, F.; Blagoev, B. Kinetics and Mechanism of the Ivanov Reaction: Reaction of Aldehydes and Ketones with Phenylacetic Acid Magnesium Enediolate. *J. Org. Chem.* **1985**, *50*, 2563−2569.
(20) Various bases derived from alkali metals or alkaline earth metals were evaluated (e.g., alkylmagnesium halides, alkyllithium reagents, or lithium amides).
(21) Full details on the flow process and the design of the flow reactor will be provided in a separate publication.
(22) On the basis of experimental results, biphenlyacetic acid (**10**) seems to act as reversible inhibitor of the transaminase enzyme CDX-043, potentially by binding to the active site, thus competing with γ-keto acid **11** as the substrate of the transamination reaction.
(23) Novick, S. J.; Dellas, N.; Garcia, R.; Ching, C.; Bautista, A.; Homan, D.; Alvizo, O.; Entwistle, D.; Kleinbeck, F.; Schlama, T.; Ruch, T. Engineering an ω-Transaminase for the Efficient Production of a Chiral Sacubitril Precursor. Manuscript submitted.
(24) For a seminal application of biocatalytic transamination in the pharmaceutical industry, see: Savile, C. K.; Janey, J. M.; Mundorff, E. C.; Moore, J. C.; Tam, S.; Jarvis, W. R.; Colbeck, J. C.; Krebber, A.; Fleitz, F. J.; Brands, J.; Devine, P. N.; Huisman, G. W.; Hughes, G. J. Biocatalytic Asymmetric Synthesis of Chiral Amines from Ketones Applied to Sitagliptin Manufacture. *Science* **2010**, *329*, 305−309.
(25) For a recent review on the use of transaminases for industrial applications, see: Kelly, S. A.; Pohle, S.; Wharry, S.; Mix, S.; Allen, C. C. R.; Moody, T. S.; Gilmore, B. F. Introduction: Biocatalysis in Industry. *Chem. Rev.* **2018**, *118*, 349−367.
(26) Isopropylamine was initially used as the corresponding hydrochloride salt, but was subsequently replaced by an aqueous solution of isopropylamine. Due to the low boiling point of isopropylamine, use of an aqueous solution significantly facilitated operations at large scale.
(27) During the initial stages of process development, buffer systems (e.g., based on phosphate or borate buffer systems) were used.
(28) Alternative approaches to shift the reaction equilibrium to the product have been described in the literature. For details, see ref 25 and references cited therein.
(29) The shift of the equilibrium towards the product is presumably driven by the lower solubility of amino acid **12** compared to γ-keto acid **11** in the aqueous reaction medium. Similar observations have been made in transamination reactions of related substrates.
(30) At 25 °C, hydrochloride salt **12** has a solubility of 105 g/L in 2-methyltetrahydrofuran (2-MeTHF) saturated with water (ca. 4−5% (m/m) water).
(31) The total carbon dioxide release (TCR) for all processes was calculated based on the process mass intensity (PMI) values, using conversion factors for all waste streams (2.3 kg CO_2/kg organic waste, 0.628 kg CO_2/kg aqueous waste). For details, see: Onken, U.; Koettgen, A.; Scheidat, H.; Schueepp, P.; Gallou, F. Environmental Metrics to Drive a Cultural Change: Our Green Eco-Label. *Chimia* **2019**, *73*, 730−736. For references on the PMI methodology, see: (a) Jimenez-Gonzalez, C.; Ponder, C. S.; Broxterman, Q. B.; Manley, J. B. Using the Right Green Yardstick: Why Process Mass Intensity Is Used in the Pharmaceutical Industry To Drive More Sustainable Processes. *Org. Process Res. Dev.* **2011**, *15*, 912−917. (b) Kjell, D. P.; Watson, I. A.; Wolfe, C. N.; Spitler, J. T. Complexity-Based Metric for Process Mass Intensity in the Pharmaceutical Industry. *Org. Process Res. Dev.* **2013**, *17*, 169−174. (c) Jiménez-González, C.; Ollech, C.; Pyrz, W.; Hughes, D.; Broxterman, Q. B.; Bhathela, N. Expanding the Boundaries: Developing a Streamlined Tool for Eco-Footprinting of Pharmaceuticals. *Org. Process Res. Dev.* **2013**, *17*, 239−246.
(32) The comparison is based on the number of distinct chemical transformations up to key intermediate **6**, starting from compounds that are readily commercially available on large scale. For the established synthetic route, the five chemical transformations required to access compound **1** (not shown in Scheme 1) are taken into account.

https://dx.doi.org/10.1021/acs.joc.0c00473
J. Org. Chem. XXXX, XXX, XXX−XXX